Chapter 4

Roller-Web Interface Finite Difference Model

The end goal of this project is to allow the correct specification of a roller-heater system given a general set of customer requirements. Often the requirements known by the application designer are the web inlet and desired outlet temperatures, and web speeds and thermal properties. Predicting the required roller size and its accessory power supply requires knowledge of the thermal interaction between the web and the roller. To predict the web heating a finite difference model of the web roller interface was written to simulate the web being heated as it passes over the roller. This chapter discusses the modeling technique as well as the approximations made in the model. The simulations done with the roller showed the relative importance of the contact resistance relative to the conduction resistance in the plastic.

4.1 Derivation and Boundary Conditions for Non-Nipped Interfaces

A non-nipped roller web interface was modeled. A non-nipped interface occurs when the web runs over one heater roller, with no top roller impinging on the plastic. Non nipped interfaces have a low interface pressure (0.5-6 kPa) as the tension on the plastic supplies all

the resultant pressure. As the modulus of elasticity of plastics is so low, especially when heated, the potential for plastic stretching and tear sets the upper limit on interface pressure. Higher pressures require the presence of a nip roller, and have much higher heat transfer rates than non nipped cases.

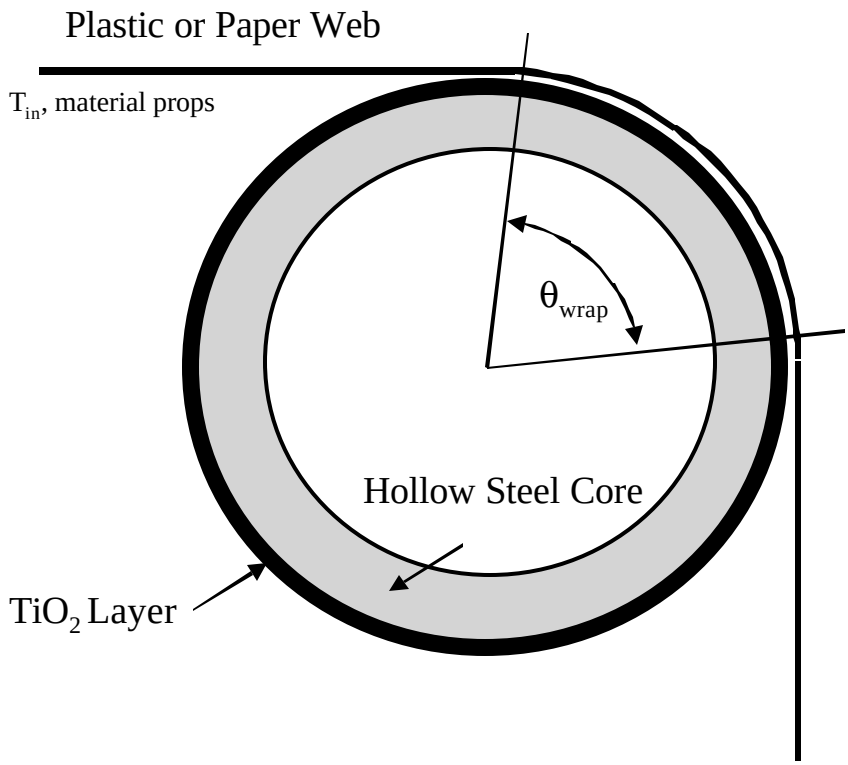

Figure 4.1.1: Considered Roller-Web System

A simple system is shown in figure 4.1.1. In the Thermalon® roller a hollow steel core is coated by plasma arc with a thin layer of titanium dioxide (TiO_2). Metallic slip rings are built on the outside of the steel core, allowing an electrical connection to the TiO_2 layer. A control circuit applies 120-480 V across the ends of the core, generating heat through ohmic dissipation. There are also thin layers of dielectric material acting as an electrical

insulator on the inside and outside of the TiO_2 layer. The electrically insulating layers are thin with negligible thermal resistance and are not considered in the thermal model. The dielectric layers prevent an electrical short circuit of the TiO_2 layer by the steel core or web material.

The plastic web and the roller are modeled using finite difference techniques. The web and roller models interact when the web is in contact with the surface of the roller, and are separate systems when the web and roller surfaces do not touch. The energy from the roller surface to the web surface is transferred through the thermal contact resistance.
The web passing over the roller has some wrap angle and based on that angle and web speed, a time in contact with the roller surface. Discretization of the energy equation provides the basis of the thermal model of the web. The heat equation's one dimensional form provides the basis for the web model:

$$\frac{\partial T}{\partial t} = a \frac{\partial^2 T}{\partial y^2} \tag{4.1.1}$$

Where α is the ratio between the energy transport in a solid to the energy storage in the solid. α is defined as:

$$\alpha = \frac{k}{\rho c_p} \tag{4.1.2}$$

The heat equation relates the energy transport from the roller to the web and the web internal energy change as the web passes over the roller. The energy absorbed by the surface of the web in contact with the roller is also conducted through the layers of the web itself.

The incremental distance the web moves during each step is converted into an equivalent timestep where the web absorbs energy from a certain position on the roller surface.

A schematic form of the finite difference grid used to model the web- roller system is shown

below.

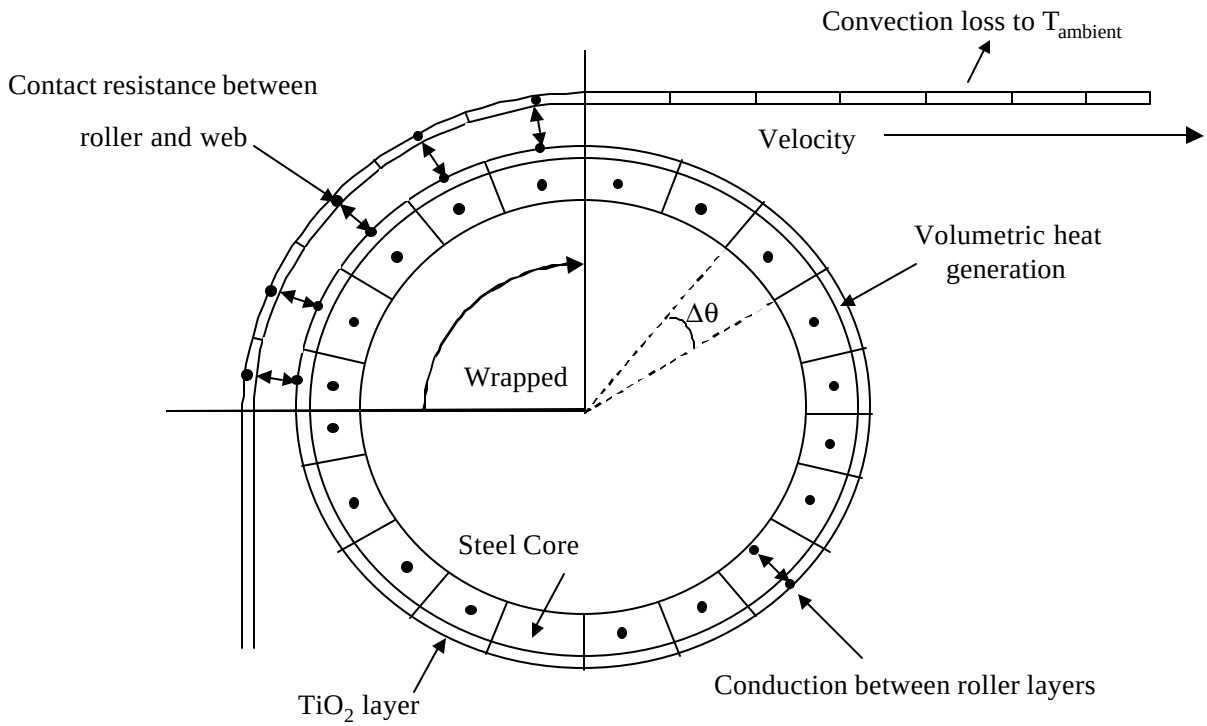

Figure 4.1.2: Finite Difference Model Used in Roller-Web Model.

The roller core and covering is modeled separately from the web as a 2-D conduction problem. There is conduction radially between the different layers of the roller, and circumfrentially around the roller. Axial variations in the roller temperature along the face are not considered. The boundary condition for the roller requires the temperature of the

nodes at the start and end of a revolution to be equal. The temperature of the nodes cool while the web is in contact with the roller and heated up again after the web leaves the surface of the roller. However the net temperature and energy change as each node goes around the cycle was zero. Thus the roller had a steady-periodic solution. As there was energy loss to the web during the revolution, the internal heat generation in the TiO_2 layer is coupled to the temperature change of the nodes. The internal heat generation completes the energy balance for the whole roller nodal system. The integration between time steps was accomplished with a 50-50 Crank Nicholson formulation.

The grid is split into two distinct sections. The area where the web contacted the roller is one section, and the area where the web is not in contact is the other section. When the web is in contact, the resistance network of the web and roller are connected by the contact resistance. There are also resistance's for convective heat loss for the sides of the web not in contact with the roller and for the roller surface while not in contact with the web. The resistance's between the layers are internal conduction resistance's. Each layer has its own thermal conductivity, specific heat and density.

A section of the model when the web is in contact with the roller is shown in figure 4.1.3 below:

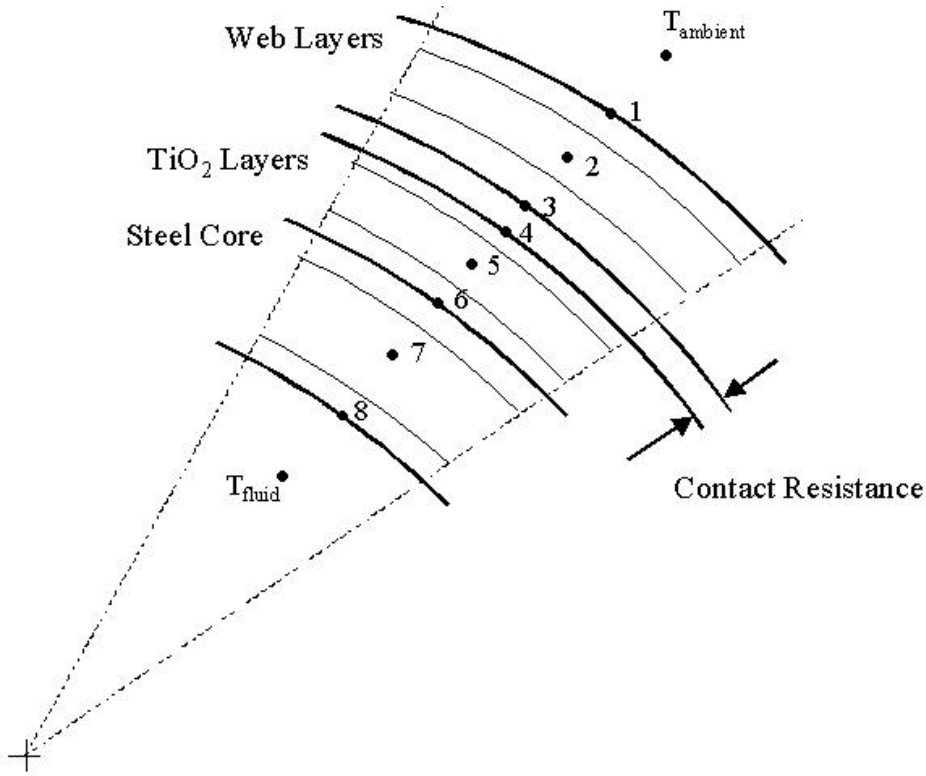

Figure 4.1.3: Finite Difference Model Section.

A generic energy balance for each radial node can be written as:

$$\frac{T_{i-1} - T_i}{R_1} - \frac{T_i - T_{i+1}}{R_2} = m_i \cdot cp_i \cdot \frac{\Delta T}{\Delta t} \tag{4.1.3}$$

Where the resistance for each node is shown in table 4.1.1 below:

	In Contact		Not in Contact	
Node #	R_1	R_2	R_1	R_2
1	$1 / h_{loss}$	$l_{node} / k_{plastic}$	$1 / h_{loss}$	$l_{node} / k_{plastic}$
2	$l_{node} / k_{plastic}$	$l_{node} / k_{plastic}$	$l_{node} / k_{plastic}$	$l_{node} / k_{plastic}$
3	$l_{node} / k_{plastic}$	$R``_{tc}$	$l_{node} / k_{plastic}$	$1 / h_{loss}$
4	$R``_{tc}$	l_{node} / k_{TiO2}	$1 / h_{loss}$	l_{node} / k_{TiO2}
5	l_{node} / k_{TiO2}	l_{node} / k_{TiO2}	l_{node} / k_{TiO2}	l_{node} / k_{TiO2}
6	l_{node} / k_{TiO2}	l_{node} / k_{steel}	l_{node} / k_{TiO2}	l_{node} / k_{steel}
7	l_{node} / k_{steel}	l_{node} / k_{steel}	l_{node} / k_{steel}	l_{node} / k_{steel}
8	l_{node} / k_{steel}	Adiabadic	l_{node} / k_{steel}	Adiabadic

Table 4.1.1: Resistance Network for Finite Difference System.

When the model is predicting the surface heat generation, a volumetric heat generation term is included in the TiO_2 layer. The model also can be switched to consider the case of traditional rollers, i.e., internally heated with a hot fluid. An inside fluid temperature and a convection coefficient would then be entered into the model. This was done to allow comparison with traditional web heating methods.

Three radial nodes are used in the web, and five radial nodes are used in the roller core and covering. In the transient space, 72 nodes are used, each representing 5 degree increments. Then number of nodes wrapped in the 360 circle is 72. The number of nodes split between the contact and non contact zones varies depending on the wrap angle. For a 180

degree wrap, half the 72 nodes, or 36 nodes, are considered wrapped. As the number of nodes had to be an integer number, the wrap accuracy is 5 degrees (360/72=5).

The model is programmed in EES, and can be used to calculate the web outlet temperatures knowing the contact resistance, or calculate the contact resistance knowing the web inlet and outlet temperatures. This is useful for both parametric studies as well as reducing experimental data. See chapter 6 of the use of the model in reducing experimental data.

The convection coefficient used in the calculations was based on published Nusselt number correlations. Two correlations are used, a rotating cylinder correlation and a flat plate solution. This was done as the exact nature of the boundary layer around the web and cylinder is not known and would have required extensive numerical solution to determine it. The heat transfer coefficient obtained from the rotating cylinder correlation is higher than from the flat plate correlation by a factor of two for a given web speed, and an average of the two is used. Due to the small distance the web travels until the exit measurement was taken, this approximation is deemed acceptable. The convection coefficient varies from 3 W/m^2-K to 25 W/m^2-K for web speeds from 1 to 10 m/s. The convection coefficient became important when reducing experimental data on the thin plastics.

4.2 Model Capabilities

The model was used to examine the heat transfer between the roller and the web, as well as the effect of different parameters on the web outlet temperature. From the numerical simulations the difference between the web contact surface temperature and the web average temperature became apparent. The web contact surface temperature was the temperature at node 3, as shown in figure 4.1.3. The web average temperature was the volume-averaged temperature of node 1, 2 and 3 in figure 4.1.3. As the web came into contact with the hot roller, the surface node (node 3) of the web absorbed energy from the surface node of the roller (node 4). The energy was then conducted through the web from node 3 to nodes 1 and 2.

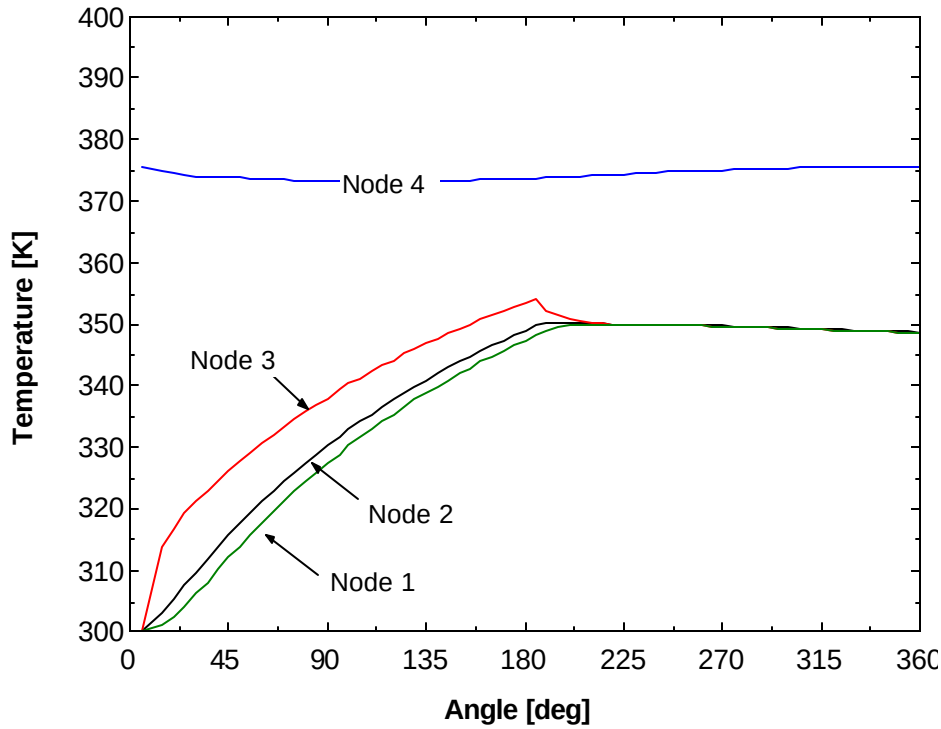

Figure 4.2.1 : Nodal Temperatures for the Roller Surface (node 4), Web Contact Surface (Node 3) and Web Middle and Outside Surface (nodes 1 and 2)

In order to calculate the web average temperature the volume average temperature of the nodes was calculated. The average temperature was found by:

$$T_{avg} = \frac{T_{node1} + 2 \cdot T_{node2} + T_{node3}}{4} \tag{4.2.1}$$

Various aspects of web heating were examined with the roller web model. In figure 5.2.2 the heating of a 0.127 mm Polyester web is shown. The web inlet temperature is 300°K, and the roller surface temperature at the measurement point is 360° K. Web speed is 0.5 m/s and the roller was spinning at 31 rpm. The contact resistance shown is the average of what was measured in the static block tests, 0.0008 m^2-K/W. A wrap angle of 180 degrees was

used on a 0.30 meter diameter roller. The power transferred to the web is 4.3 kW/meter of contact width.

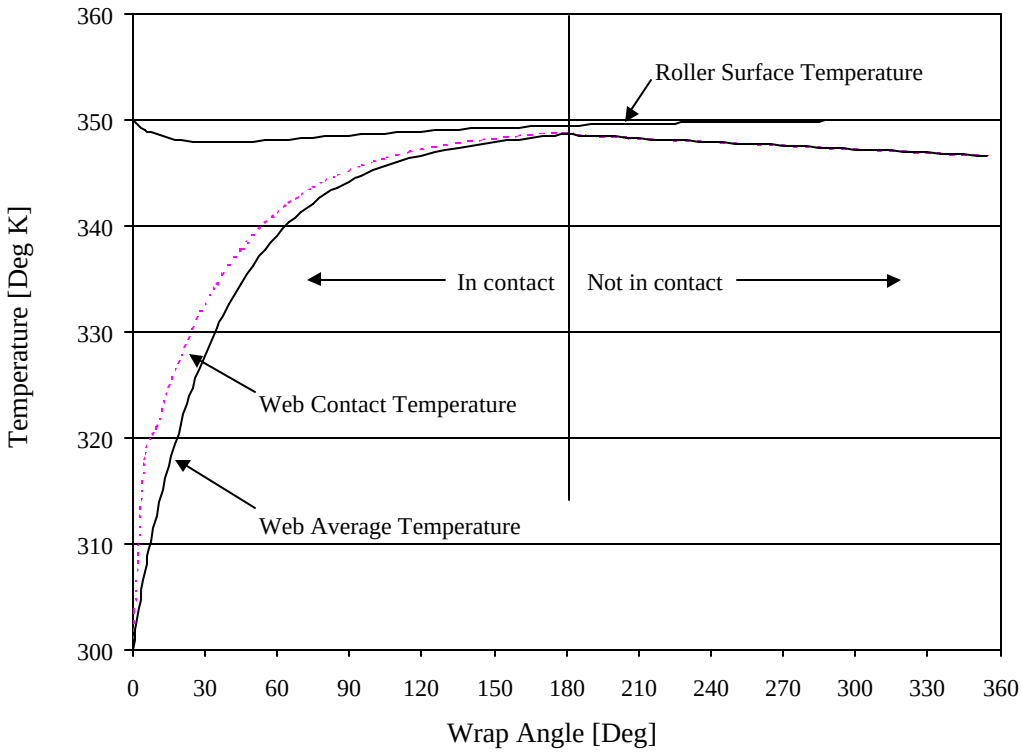

Figure 4.2.2: Predicted Heating of 0.13 mm Polyester Web. R_{tc} = 0.0008 m^2-K/W.

The temperature of the web rises while in contact with the roller, and then slowly cools off due to convective losses. Two web temperatures are shown, the temperature of the node in contact with the roller, and the average web temperature. The temperature of the side of the web in contact with the roller heats up faster then the bulk web temperature, and then the heat is conducted to the other parts of the web. The temperature difference between the contact node and the average temperature is more significant the thicker the web.

The roller temperatures at zero degrees and 360 degrees are the same. The roller temperature was fixed by setting node 4 to the nominal roller temperature. Node 4 was fixed at a wrap angle of 270 degrees. This location was chosen as it was where the temperature of the roller was measured during the experimental tests. As the roller temperature is controlled based on the measurement temperature, it was deemed the best reference point. The rest of the roller node temperatures are allowed to float based on the thermal loading of the web. The lowest surface temperature of the roller occurs after the greatest heat gain by the web. As the web is heated up closer to the roller surface temperature, less heat was transferred to the web. As the internal heat generation in the TiO_2 layer is assumed constant, the roller then heats up after the web leaves contact. In all of the tests run, the temperature variation in the roller surface as the roller passes through a rotation is typically less than 3°K, and for the majority of the tests, less than 2°K.

The effect of web thickness on the thermal profile of the web was substantial. Figure 5.2.3 shows a 0.508 mm thick web of PVC under the same conditions as shown above. Whereas the temperature rise of the Polyester web above was almost 48°K , for the PVC it is much less, approximately 38°K. The temperature gradient between the web layers is also more substantial. In the polyester case, the average web temperature was very close to the contact temperature for the web. The PVC contact temperature is substantially hotter (18° K at the end of contact) than the PVC average temperature, before the energy is conducted to the rest of the roll.

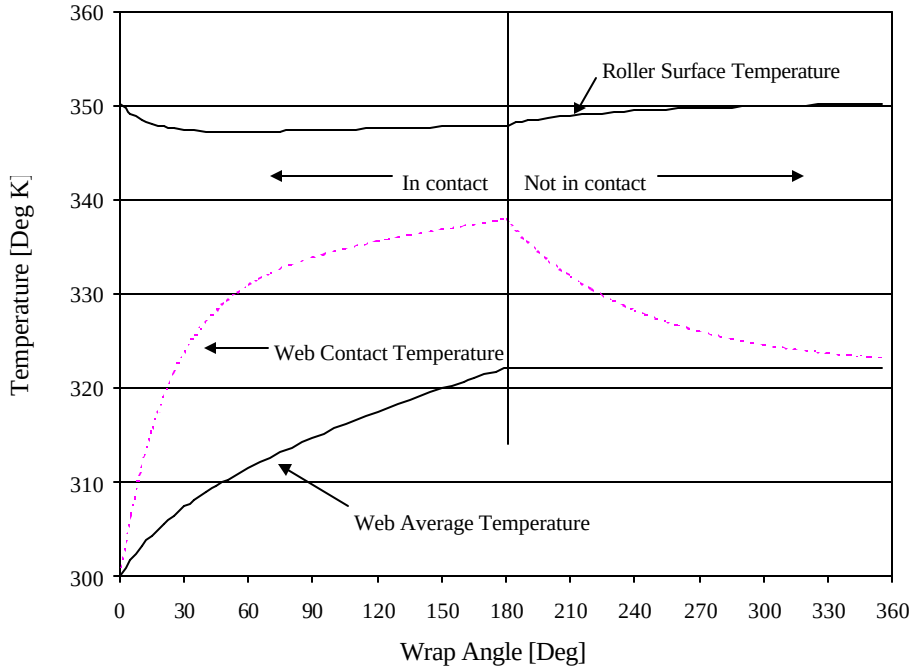

Figure 4.2.3: Predicted Heating of 0.508 mm PVC Web. R_{tc} = 0.0008 m^2-K/W.

After the web leaves the roller, the predicted web contact temperature drops quickly, while the average web temperature does not. This is due to heat conduction through the layers. The energy in the hot nodes is redistributed through the remaining layers. As the relatively thick PVC has a high thermal capacitance rate, the average web temperature cools very slightly due to convective losses. Although the web temperature rise for the PVC is not as high as in the polyester case, the power delivered to the web is much greater, at 10.2 kW/meter contact width vs. 4.6 kW/meter for the polyester web.

4.3 Transient Capacity Effects

As shown in the figure 4.2.1 and 4.2.2, the web will not reach the temperature of the roller even at slow speeds and high wrap angles. The energy exchange between the roller and the web is a transient process, and the transient conduction effects in the web must be considered. The transient effects in web processing vary with the different process parameters of web and roller temperatures, web speeds, wrap angle, and web thickness. In general, the process parameters vary two things, the capacitance rate of the web, and the potential for heat transfer from the roller to the web.

The capacitance rate of the web is a quantitative measure and it is defined as;

$$Ca\dot{p} = \dot{m}_{web} \cdot c_p \tag{4.3.1}$$

It is equal to the capacitance rate found in heat exchanger technology. The heat transfer potential is a qualitative measure that is a function of the temperature difference across the web roller contact zone and the time that the web and roller are in contact.

Through the rest of the chapter, a web heating effectiveness is used. Due to the different operating temperatures and web inlet temperatures, this effectiveness is used to combine the effects of different web inlet and roller heater temperatures. The effectiveness is a measure of how well the roller heated the web given the inlet temperature of the web and the roller.

The dimensionless effectiveness is defined as:

$$\varepsilon = \frac{T_{web,out} - T_{web,in}}{T_{roller} - T_{web,in}} \tag{4.3.2}$$

The importance of this effectiveness is shown in figure 4.3.1 and 4.3.2, below. For both the 0.127 mm Polyester and 0.508 mm PVC, the web outlet temperature is plotted as a function of $R_{tc.}$ Different roller temperatures are used, and the web outlet temperatures are shown. When the effectiveness is calculated for each of the different roller temperatures and contact resistances, the effectiveness curves collapse into one curve, shown in figure 4.3.3. The variance in the effectiveness' for the three roller temperatures was less than 0.1%. This is true for both plastic samples.

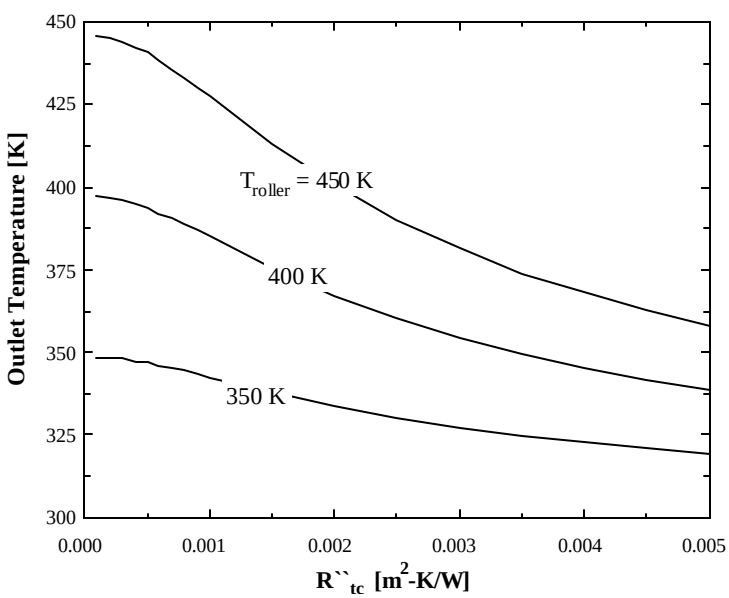

Figure 4.3.1: Effect of Contact Resistance on Web Outlet Temperature

In figure 4.3.1, the web outlet temperature of a 0.13 mm polyester sample is shown for three different roller temperatures, 450°K, 400 °K and 350 °K. The contact resistance was varied over the ranges encountered in the static block tests. As expected, the lower the contact resistance, the higher the web outlet temperatures. The sensitivity of the outlet temperatures to the contact resistance varies according to roll temperature.

For each of the different roll temperatures, the calculated effectiveness based on the web outlet temperature and roll temperature collapses into one line. This proves the validity of the effectiveness concept for comparison purposes. The effectiveness however cannot be used to predict the web outlet temperatures for different plastics or the same plastic at different wrap angles. It does however simplify the different temperature ranges that could be considered.

A similar trend in the effectiveness is shown in figure 4.3.2 below. 0.508 mm PVC plastic is used in the simulations. The calculated effectiveness is much lower than the polyester case, due to the greater capacitance rate encountered by the heater roller. For both of the plastic runs, the web speed and wrap angle were 1 m/s and 180 degrees, commonly encountered values in processing.

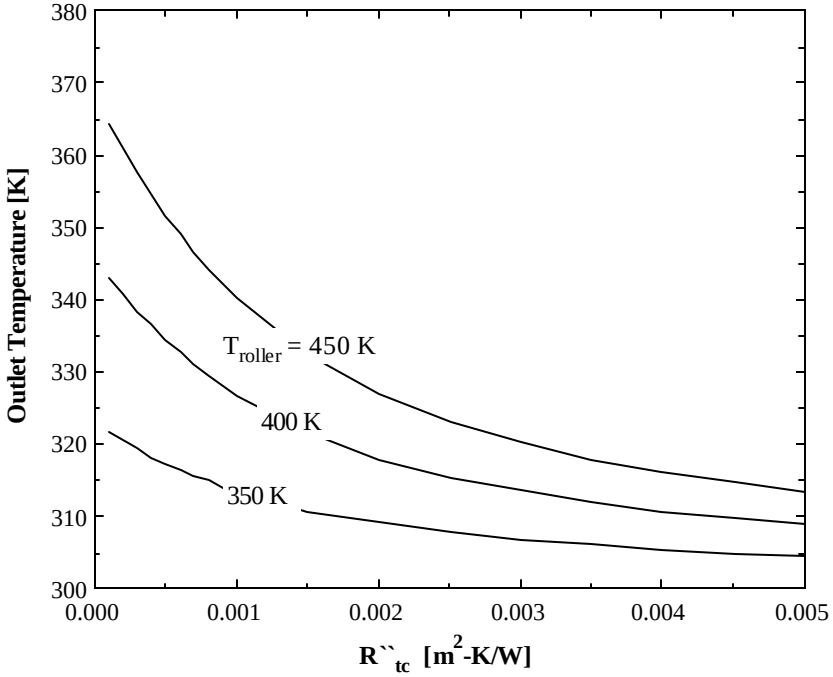

Figure 4.3.2: Calculated Web Outlet Temperatures for 0.508 mm PVC

The calculated effectiveness for the above polyester and PVC runs collapse into similar lines for all of the temperatures (Figure 4.3.3). The predicted effectiveness for the polyester and the PVC samples are different, but the calculated effectiveness were the same for the different roller temperatures of each plastic. The effectiveness curves are shown in figure 4.3.3.

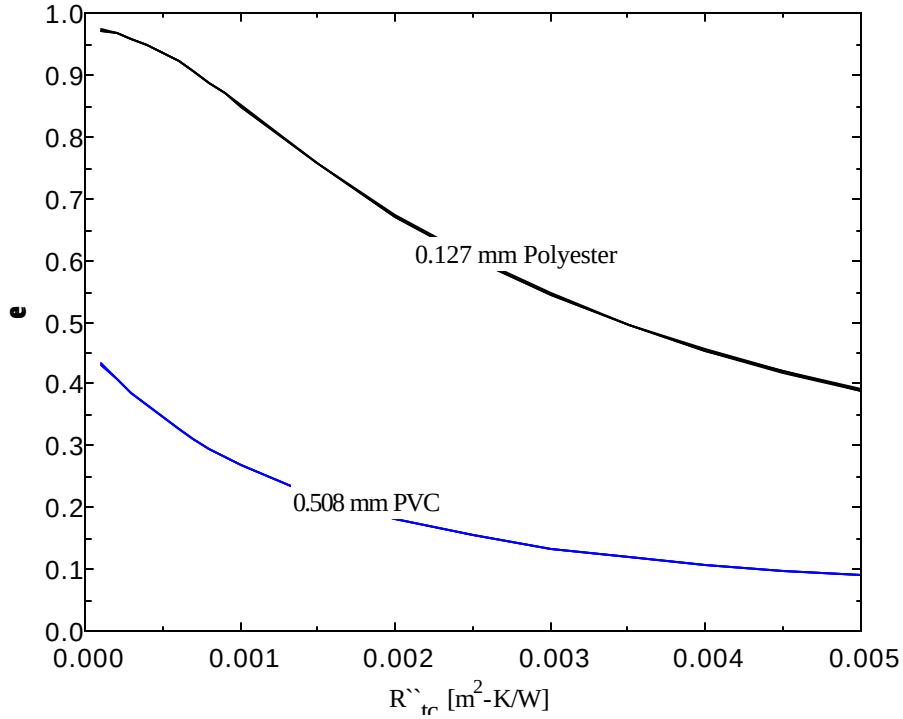

Figure 4.3.3: Calculated ε for PVC and Polyester

At contact resistances less than 0.0010 m^2-K/W, the contact resistance has a small effect on the predicted effectiveness. This implies that the surface of the plastic that is in contact with the roller reaches the roller temperature, and the limiting resistance to heat flow is in the conduction resistance in the plastic web.

The effectiveness parameter is used to examine the effect of various parameters on thermal web processing. The relative effects of varying web speed and wrap angle are looked at for each of the plastics. The effect of varying plastic thickness was examined for the polyester plastic, with a comparison to the PVC sample as well. Unless otherwise noted all wrap angles are 180 degrees over a 0.30 meter roller.

Figure 4.3.4 shows the effect of web speed on the 0.127 mm Polyester. Higher web speeds produce a lower heating effectiveness. At the slowest web speed considered, 0.5 m/s, the contact resistance has little effect until about 0.001 m^2-K/W. At a contact resistance higher than 0.001 m^2-K/W, the contact resistance has a much larger effect on the effectiveness. At the higher speeds in the graph, the effectiveness is lower. By 0.0030 m^2-K/W, which was the average of the contact resistance encountered in the embossed samples, the contact resistance had a very small effect on the calculated effectiveness.

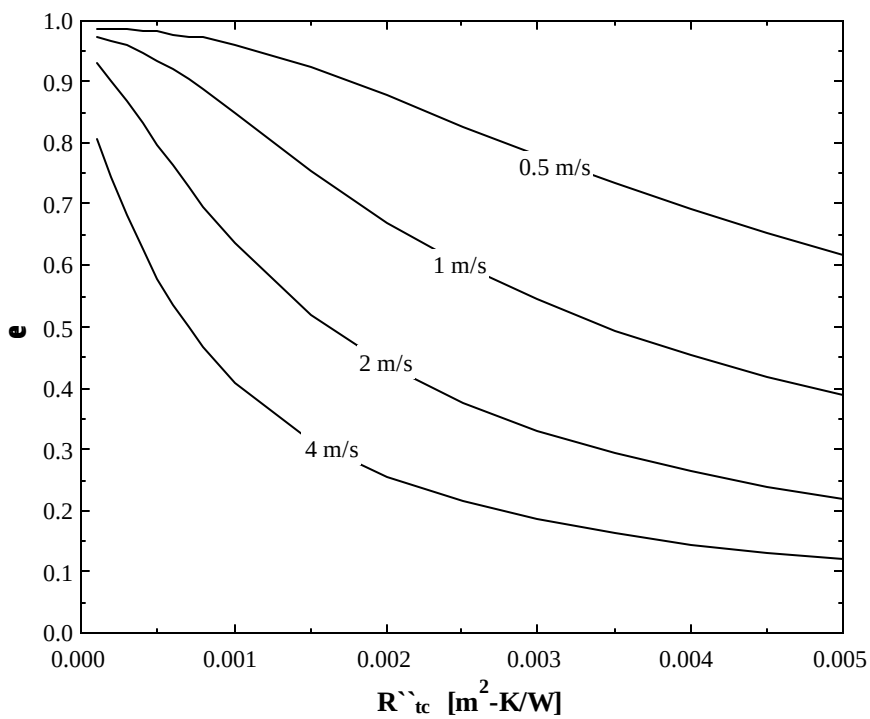

Figure 4.3.4: Calculated ε for Polyester with Varying Web Speeds

Similar trends are encountered when the web speed was varied with the 0.508 mm PVC (figure 4.3.5). The effectiveness is in general lower, and the higher the web velocity, the lower the effectiveness.

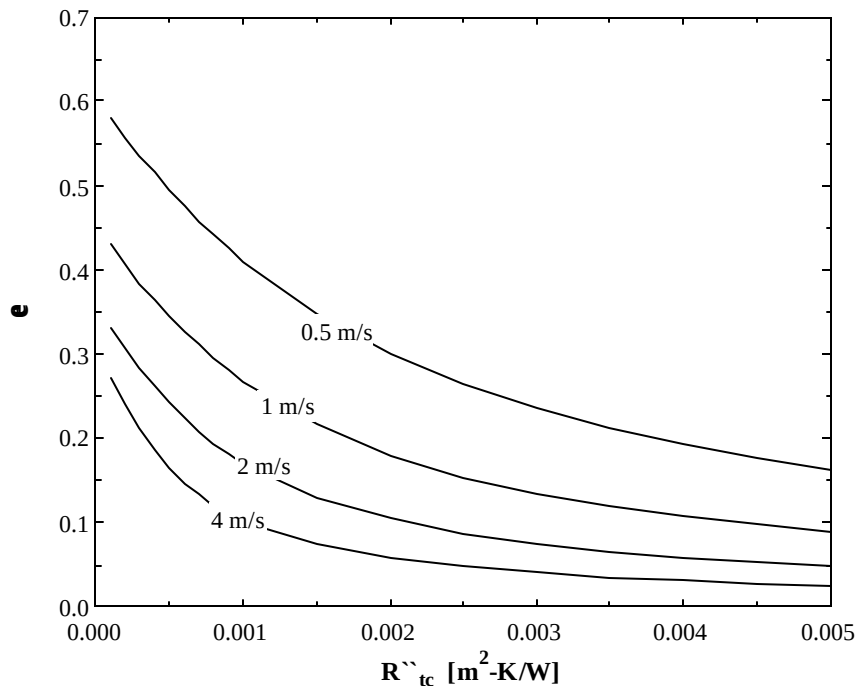

Figure 4.3.5: Calculated ε for PVC with Varying Web Speeds

Decreasing the wrap angle and a similar effect as increasing the web speed, it decreased the process effectiveness. Decreasing the wrap angle decreased the contact time, and the corresponding potential for heat transfer. Figure 4.3.6 shows the effect of varying the wrap angle on the 0.127 mm polyester sample.

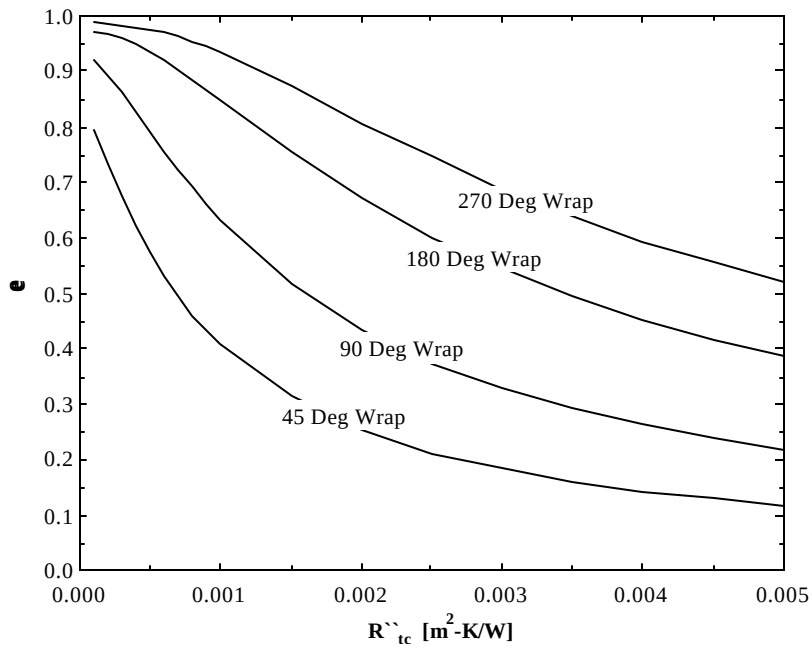

Figure 4.3.6: Calculated ε for Polyester with Varying Wrap Angles

There was a similar effect on the 0.508mm PVC. Due to the low heat transfer of most runs, the contact resistance has a low effect on the processing effectiveness, and the effectiveness curves in figure 4.3.7 flatten out at contact resistances greater than 0.003 m^2-K/W.

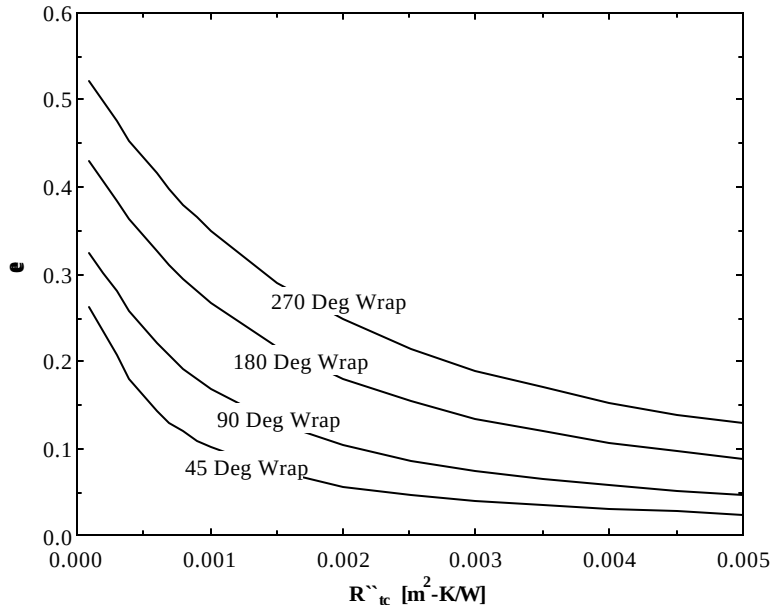

Figure 4.3.7: Calculated ε for PVC with Varying Wrap Angles.

All of the above comparisons are between two different plastics, each with different specific heats, conductivity and density. The greatest difference is in the thickness however, with the polyester sample having a thickness of 0.127 mm and the PVC sample having a thickness of 0.508 mm. A final comparison was made between thickness' of the same plastic, in order to show the effect of` web thickness.

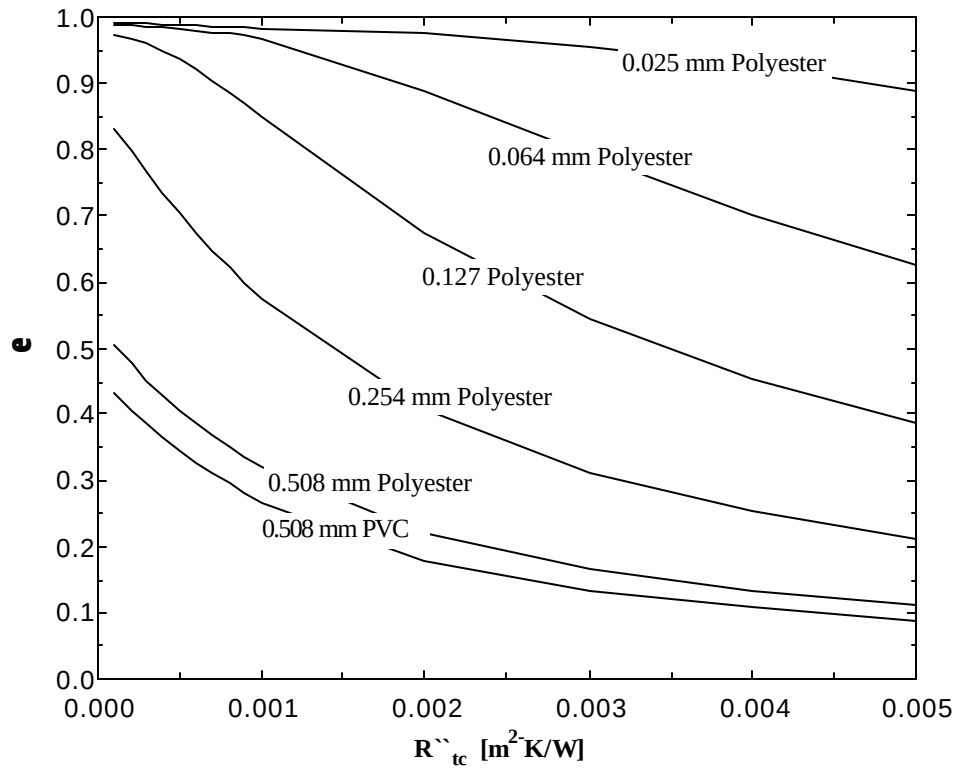

Figure 4.3.8: Calculated ε for Polyester of Varying Thickness

Also shown is the predicted effectiveness for 0.508 mm PVC under the same conditions. The difference in the calculated effectiveness for the two materials is due to the property variations between the materials. Trying to predict the difference based on heat transfer principles is hard however. The average difference between the calculated effectiveness for the 0.508 mm PVC and the 0.508 mm polyester sample was 16%.

The specific heat-density product difference was 27%. As the problem is transient, steady state parameters cannot fully describe the difference. Transient calculations are usually governed by the thermal diffusivity parameter.

The difference in the thermal diffusivity for the two plastics was 46%, with the polyester having the higher diffusivity. This was much larger than the difference in the effectiveness between the two cases, and shows the non-linearity in the transient process.

4.4 Thermalon® vs. Internally Heated Rollers

The Thermalon® roller technology developed by American Roller Company has several advantages over conventional internally (convectively) heated rollers. All stem from the fact that because the heat is generated where it is used and can be measured, control of the heater roll is much easier. A comparison of the thermal gradients through the roller cores in the two technologies was made possible with the finite difference model that could simulate both cases. An analysis is done between two roller systems supplying the same thermal energy to the web at the same nominal contact temperature. The difference in the two technologies becomes readily apparent.

In the Thermalon® case, the surface temperature varies based on its contact with the web. Figure 4.4.1 shows the contact surface, the inside surface, and the middle node temperature of the roller heating the web. The contact surface temperature is generally below the inside surface temperature while in contact with the web, and generally above when not in contact with the web. The inside temperature is essentially constant and is unaffected by the heat loss to the web. The temperature of the middle node varies between the two extremes set by the contact and inside surface temperatures.

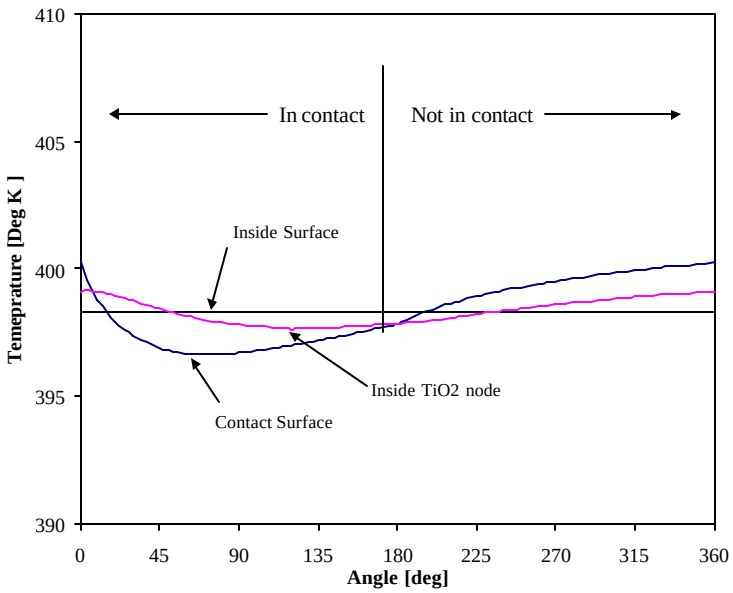

Figure 4.4.1: Surface Temperature Distribution for Surface Heat Generation

The vastly different temperature profile for the in the internally heated roller is shown in figure 4.4.2. As the heat must be first convected from the fluid to the inside surface and then conducted from the inside of the roller through the thickness of the steel core, there is a temperature drop from the fluid temperature to the roller surface. The temperature drop is based on the energy delivered to the web, and the thickness and the conductivity of the steel core. Figure 4.4.2 shows the contact surface and internal surface temperatures under similar loading as figure 4.4.1. The surface temperature varies while in contact with the web, as with the internal heat generation case, and by roughly the same amount.

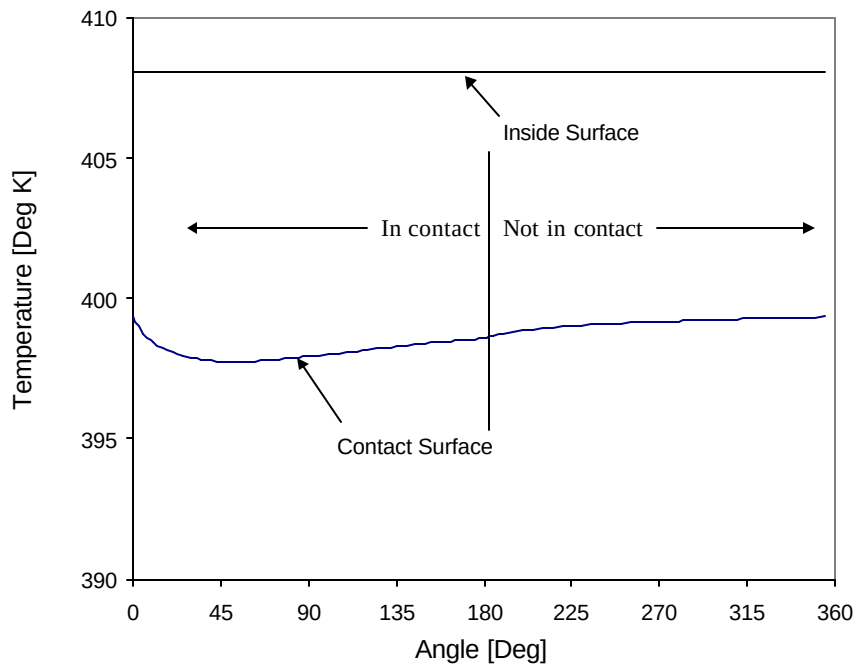

Figure 4.4.2: Surface Temperature Distribution for Convective Heat Generation

The hot fluid supply temperature must be higher then the inside surface temperature, but the actual supply temperature is based on the amount of energy supplied to the web and the internal convection coefficient. Estimating the internal heat transfer coefficient is based on the expected behavior of the fluid inside the roller. The fluid behavior is dependent on both roll speed and the amount of condensate (assuming steam is used inside as the hot fluid) inside the roller shell.

A simple analysis using a Nusselt number correlation for a rotating cylinder predicted a convection coefficient of roughly 1000 W/m^2-K. This gave a supply temperature needed between 420 – 425° K. For this example the supply temperature needs to be 20-30° K above

the roll surface temperature and 40-50 K° above the desired web outlet temperature. Controlling the web outlet temperature involves varying either the mass flow rate of condensate through the roller or the temperature of the fluid, with a large time lag in the resultant web outlet temperature.

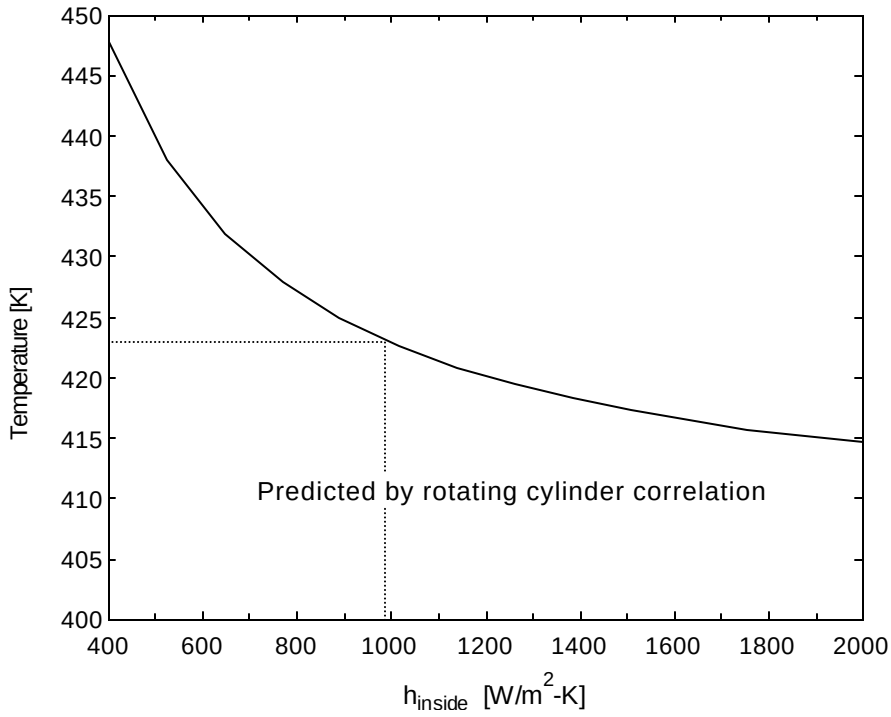

Figure 4.4.3: Required Fluid Temperature vs. Internal Convection Coefficient. Based on 15 kW/m load

If the hot fluid passing through the conventionally heated roller is steam, usually condensation occurs. Three states of common condensate behavior have been labeled by White and Higgens (1958) and Wilhelmsson (1995). The three operating regimes are; low speed puddling, medium speed cascading and high speed rimming. Low speed puddling is where the condensate simple sits in the lowest part of the hollow spinning shell. Cascading

occurs when the condensate is lifted up inside the drum due to viscous forces. Rimming occurs when a thin film of condensate is drawn all the way around the inside of the rotating roller. This increases the heat transfer to the shell and ultimately to the product. The actual convection coefficient found in the roller would depend on the condensate behavior, which is hard to predict. Therefore any comparison has to have parametric consideration of the heat transfer coefficient.

The higher energy losses from an internally heated roller result from the higher supply temperature, and also the energy loss in the fluid transport in pumps, piping etc. The combustion efficiencies in the boiler etc. would also have to be considered and would be substantial. Internally heated rollers would be thermodynamically advantageous where there is large volumes of waste heat available, but the control system and the necessary heat exchangers would counteract the lower energy cost.

4.5 Empirical Approximations

In the course of developing the full finite difference a model, a correlation was developed that gave close approximations to the finite difference model's predicted effectiveness. The advantage of the correlation is primarily convenience and speed. The correlation developed can be used on a handheld calculator, or quickly programmed into any computer programming language or spreadsheet. It can be used with different material properties, including those encountered in paper and plastic processing.

The correlation predicts the web heating effectiveness of the roller, as defined in eq. 4.3.2. A capacitance rate of the web travelling over the roller is defined as:

$$ca\dot{p} = \dot{m}_{web} \cdot c_{p,web} \tag{4.5.1}$$

Where:

$$\dot{m}_{web} = L_{web} \cdot \dot{v}_{web} \tag{4.5.2}$$

The correlation has three dimensionless parameters, C_1 C_2 and C_3. C_1 is a measure of the potential for web temperature rise of any roller web interface, and is defined as:

$$C_1 = \frac{contact_{length}}{ca\dot{p} \cdot R''_{tc}} \tag{4.5.3}$$

C_2 is equivalent to the Biot number for the web passing over the roller. It is defined as the ratio of the resistance to heat flow internal to the web to the resistance to heat flow from the roller to the web:

$$C_2 = \frac{L_{web}}{k_{web} \cdot R''_{tc}} \tag{4.5.4}$$

The correlation for the web heating effectiveness is completely empirical and takes the form of:

$$e = 1 - \exp\left(\frac{-C_1}{1 + C_3 \cdot C_2}\right) \tag{4.5.5}$$

C_3 is a curve fit parameter that varied with web speed. After minimizing the error between the effectiveness predicted by the finite difference code and the above correlation in parametric studies, it is recommended that:

$$C_3 = \frac{0.74}{\sqrt{1 + v_{web}}} \tag{4.5.6}$$

Where v_{web} is in meters per second. Alternatively a value of C_3 of 0.5 gives a close approximations in most processing cases. Figure 5.1.1 shows a comparison between the optimized value of C_3 vs. web speed and contact resistance for 0.127 mm polyester. The roller used in the study is an externally heated 0.30 m outside diameter roller.

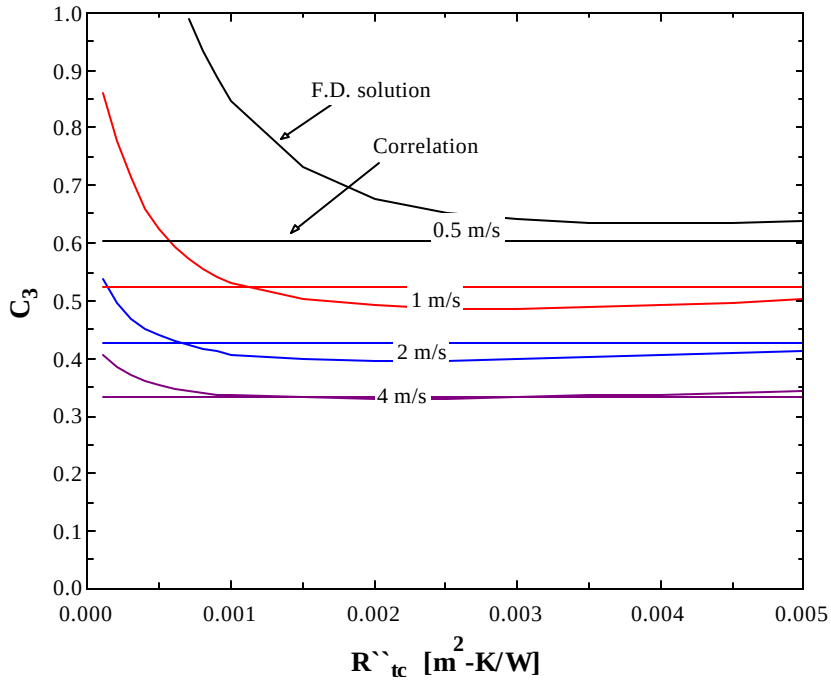

Figure 4.5.1: Finite Difference 'Best Fit' and C_3 Approximation for 0.127mm Polyester.

The curved lines are the value of C_3 needed to make the value of epsilon predicted by equation 4.5.5 exactly equal to the value calculated by the finite difference code. The straight horizontal lines are the value of C_3 predicted by equation 4.5.6. As equation 4.5.6 is based solely on web speed, the value does not change with contact resistance.

The closeness of the approximation and that predicted by the finite difference code is within the error most measurement techniques. An examination of how speed, wrap angle and web thickness affect the approximation is now examined. Figure 4.5.2 shows the effect of web speed on the closeness of effectiveness predicted by the finite difference code and equation 4.5.5.

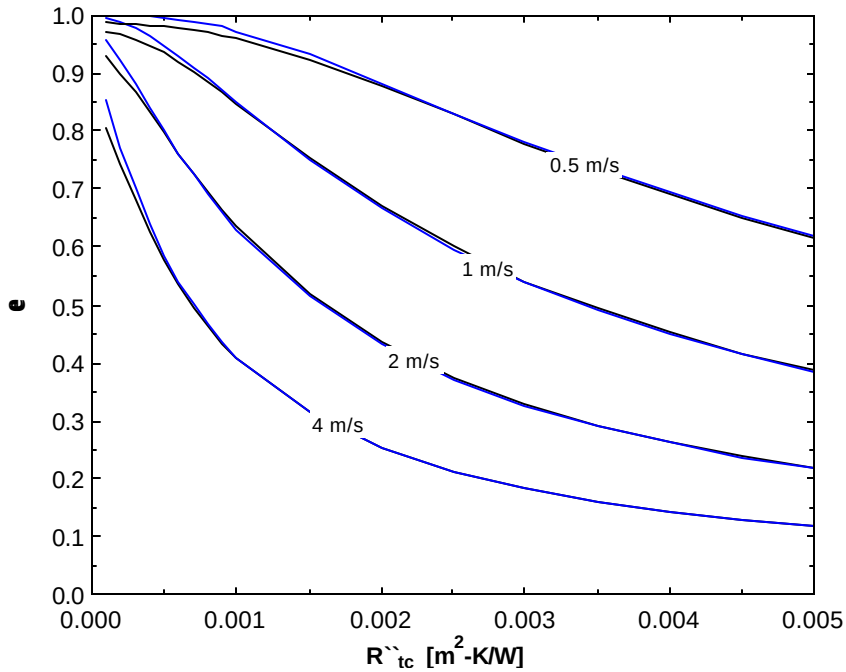

Figure 4.5.2: Comparison of Finite Difference and Correlation ε for Different Web Speeds. 0.127 mm Polyester Sample. 180 Deg Wrap Angle.

Over the range of contact resistances and web speed encountered in this study, the correlation compares well with the finite difference code. It is not as accurate at the low contact resistances in the 0.0001 to 0.0005 m^2-K/W, but over the rest of the ranges for all of the speeds it matches well.

The effect of varying the wrap angle on the accuracy of the effectiveness correlation is shown in figure 4.5.3. The effectiveness predicted at wrap angles of 45, 90, 180 and 270 degrees are shown.

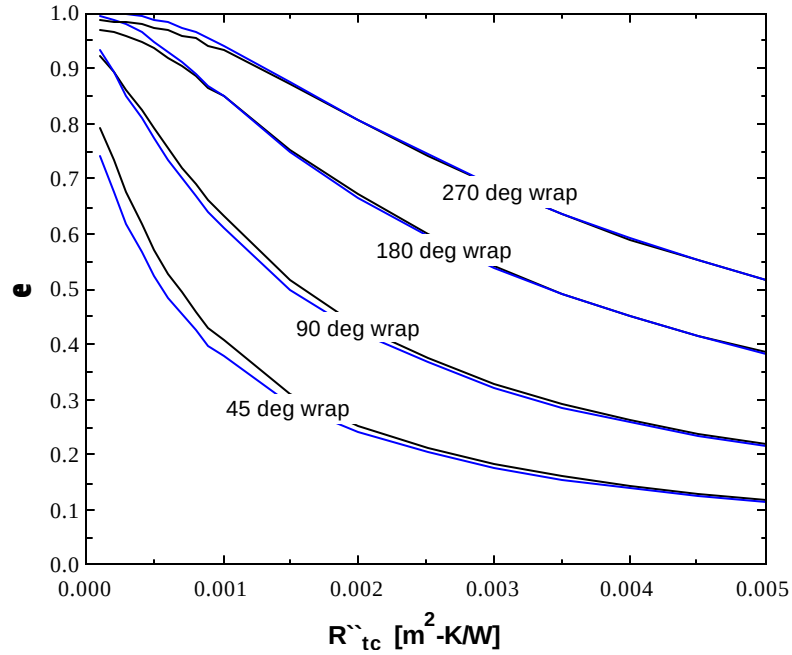

Figure 4.5.3: Comparison of Finite Difference and Correlation ε for Different Wrap Angles. 0.127 mm Polyester Sample. 1 m/s web speed.

The correlation matches quite well, except for the 45 degree wrap angle. At the 45 degree wrap angle and the low contact resistance's, the correlation differs from the finite difference code in its prediction of the effectiveness by 8 %.

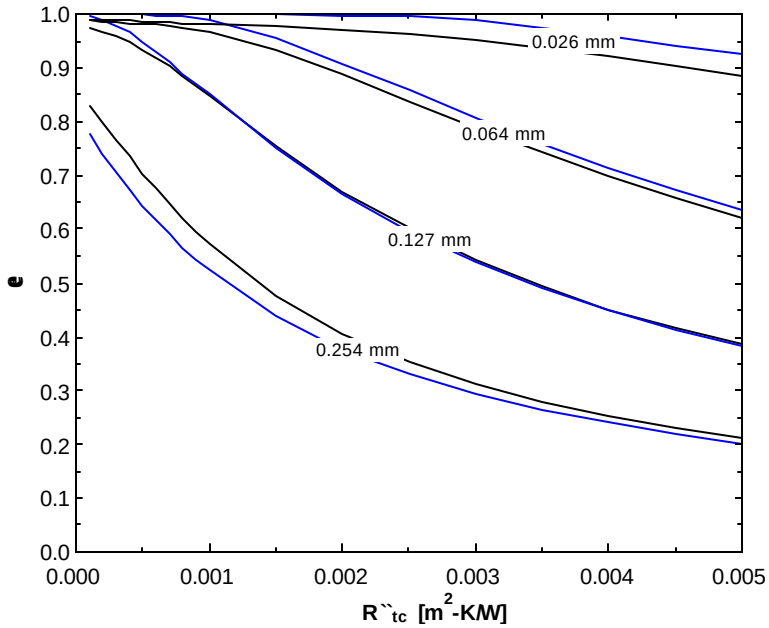

Figure 4.5.4: Comparison of Finite Difference and Correlation ε for Polyester Thickness. 180 Deg Wrap Angle. 1 m/s web speed.

Equation 4.5.5 has two important weaknesses. The first is that the correlation solely predicts the web average temperature, and does not recognize the temperature differences across the thickness of the web. The correlations' second weakness is that it does not take into account the variance in the roller surface temperature. The extent of the errors in the prediction of epsilon due to each of the above two factors is not known. The correlation is valid for both internally heated and surface heat generation rollers, but care must be taken not to exceed its design conditions.

The finite difference model developed in this section was used extensively to calculate the contact resistance found during dynamic tests using a pilot scale roller web system. Those tests are explained in the next chapter.